REPORT: 2018 SCEC Proposal

Incorporating the effects of hydrous phases and strain localization into seismic-velocity-based models for the Community Rheology Model

PIs – Greg Hirth (Brown University) and Mark Behn (WHOI; now at Boston College)

Summary, Motivation and Background

We extended our analysis of correlations between seismic velocity (P and S wave) and effective viscosity to include the influence of weak hydrous phases (e.g., micas) and the role of fabric on strain localization. As in earlier analyses on anhydrous rocks (*Shinevar et al.*, 2015), we follow a three-step approach. First, we calculate equilibrium mineral assemblages and seismic velocities for a global compilation of lower crustal rocks at various pressures and temperatures relevant for the mid- to lower crust in Southern California (using Perple X; *Connolly*, 2009). Second, we use rheological mixing models and single-phase flow laws for major crust-forming minerals to calculate aggregate viscosity for the predicted equilibrium mineral assemblages following *Huet et al.,* (2014). Third, we fit the viscosity calculations to the seismic velocity calculations for the same lithology. Using input from the SCEC Community Velocity Model (CVM), our methodology provides an independent constraint on crustal viscosity in Southern California (**Figure 1a**). A focus of these calculations was including the potential rheological effects of modest amounts of hydrous mineral phases, which are known to be present in rocks from Southern California (e.g., **Figure 1b**) and processes that lead to strain localization. Inclusion of hydrous phases is particularly
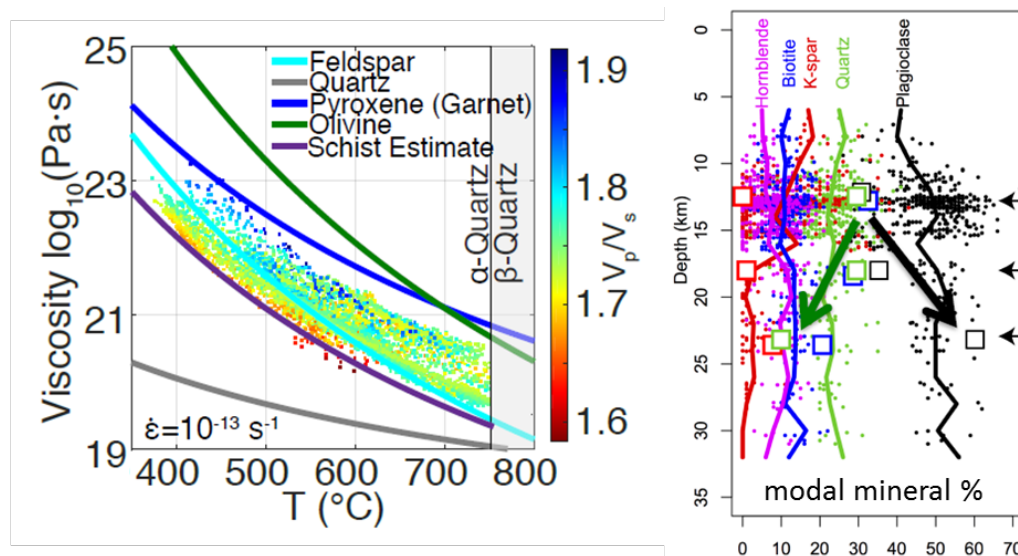

Figure 1: (a) Data points represent calculated viscosity from our correlation with seismic velocity evaluated with the SCEC CVM and thermal model for a strain rate of 1e-13/s (*Shinevar et al.*, 2018). Points are colored by Vp/Vs. Solid lines represent predicted viscosities for quartz (gray; *Hirth et al.*, 2001), plagioclase (light blue; *Rybacki et al.*, 2006), pyroxene (dark blue, *Dimonav and Dresen*, 2003), and olivine (green; *Hirth and Kohlstedt*, 2003). The purple line represents the prediction for the viscosity of biotite schist with the average mode of the Pelona-Orocopia-Rand (POR) schists, assuming an isotropic phase distribution. (b) Modal mineralogy of the Southern Sierra exhumed crustal section (dots; compiled from *Chapman et al.*, 2012) and the modes of the POR schist (boxes); Mica phase for the schist varies with depth, with muscovite and chlorite at lower greenschist grade (top arrow); biotite and phengite for upper greenschist (middle arrow); and biotite for lower amphibolite conditions (bottom arrow). Figure from discussion of the Geologic Framework (GF) for the CRM (*Oskin et al.*, SCEC Workshop 2017).

pertinent given that the Geologic Framework for the CRM in the Mojave region highlights the importance of biotite (e.g., *Oskin et al.*, SCEC CRM Workshop talk, 2017). Further, our modelling strategy provides a methodology for exploring the potential the rheological effects of fabric formation and grain size evolution on strain localization.

Results from our work in 2018

Using our approach for estimating the viscosity in isotropic rocks, we predicted the depth to the brittle-ductile transition and compare that with independent estimates for the seismic locking depth across Southern California (*Shinevar et al.*, 2018). In **Figure 2** we show the predicted depth to the brittle-ductile transition defined as the depth where the stress calculated by our method (at a given strain rate) becomes less than the strength predicted for a strike slip fault with a friction coefficient of 0.6 assuming a hydrostatic pore-fluid pressure gradient (e.g., *Zoback & Townsend*, 2001). The seismic locking depth is estimated as the depth above which 95% of earthquake epicenters occur for grid points with 30 or more
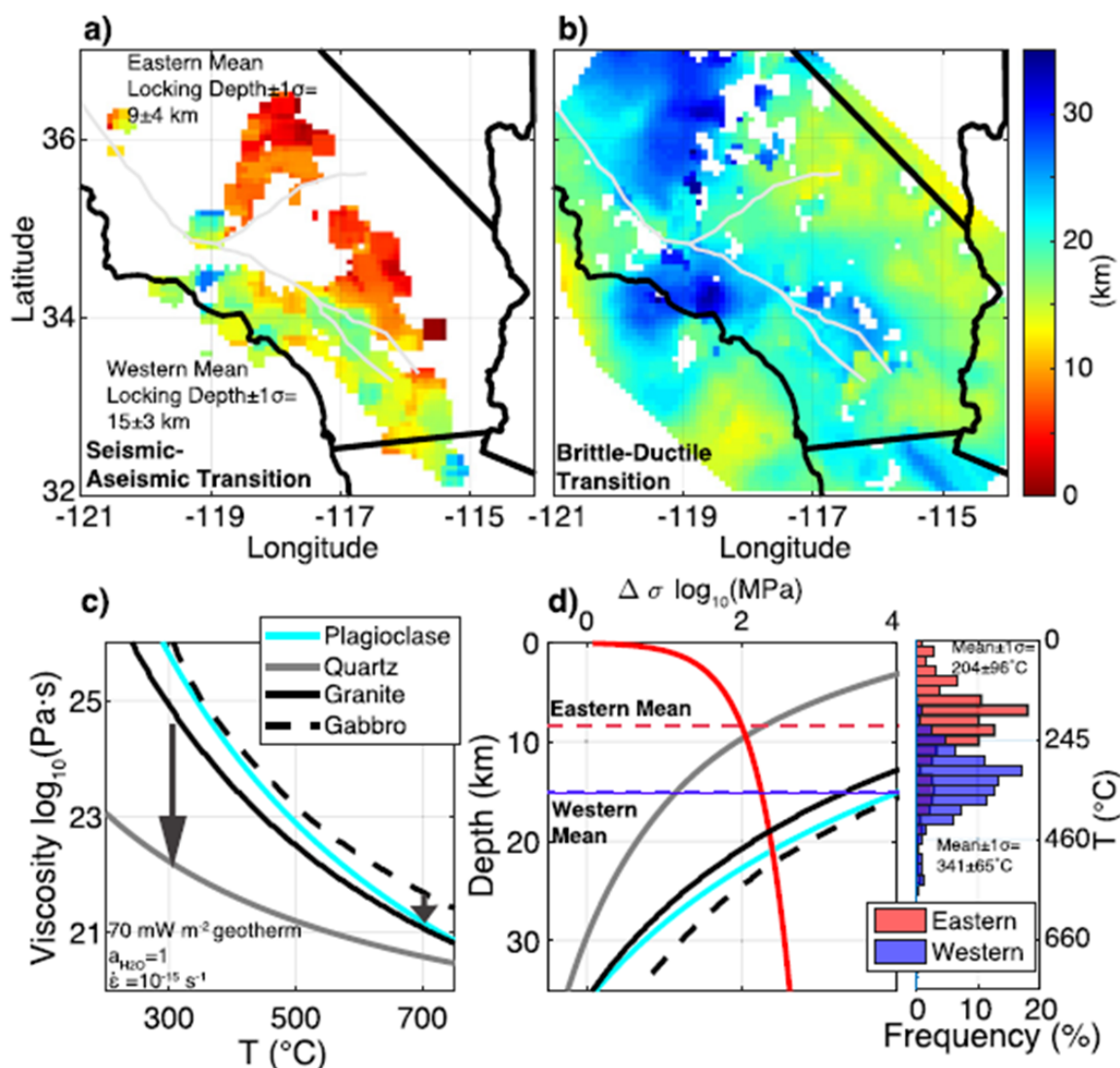

Figure 2: (a) Regional seismic-aseismic transition. (b) Predicted brittle-ductile transition. (c) Viscosity versus temperature (depth) for a 17°C/km geotherm for dislocation creep of quartzite, plagioclase, and calculated aggregate viscosities for granite and gabbro. Black arrows illustrate potential rheologic effect of fabric formation during weakening of granite and gabbro to produce interconnected quartz and plagioclase, respectively. (d) Diagram showing: (i) stress versus depth for the same flow laws in (c); (ii) mean locking depths; and (iii) locking depth temperature for regions east (red) and west (blue) of the SAF.

magnitude >3.0 earthquakes in a 15 km radius from each grid point (using only A and B quality events in the Southern California Earthquake Data Catalog (http://scedc.caltech.edu/eq-catalogs/).

Figure 2 shows distinct bimodality in the locking depth across the San Andreas Fault; with values of 8.6 ± 4.4 km (one standard deviation) east of the SAF, and 15.1 ± 3.1 km west of the SAF. The average temperature (based on our thermal calculations) at the depth of the calculated brittle-ductile transition is ~480°C for both regions (Figure 2c and d). However, the temperature at the locking depth varies significantly; the mean locking depth temperature is ~140°C lower east of the SAF than west of the SAF. We hypothesize that this difference arises from lithological variations, consistent with interpretations from *Hauksson and Meier* (2018). Specifically, for more felsic compositions (east of the San Andreas Fault, North American Plate) the locking depth may be controlled by a quartz rheology (Figure 2f), whereas for a more mafic composition (west of the San Andreas Fault, Pacific Plate) the locking depth may be controlled by a stronger plagioclase rheology. This difference suggests that the locking depth reflects strain localization controlled by the weakest phases in the rock. Thus, while the "bulk" aggregate viscosity of two lithologies may be similar (compare the solid and dashed black lines in Figures 2e and 2f), rocks with a significant fraction of quartz can be dramatically weaker if the fabric produced by deformation allows geometric percolation of the weak phase (c.f., *Tullis et al.*, 1991; *Handy et al.*, 1994; *Gerbi et al.*, 2015).

References

Chapman, A. D., Saleeby, J. B., Wood, D. J., Piasecki, A., Kidder, S., Ducea, M. N., & Farley, K. A., Late Cretaceous gravitational collapse of the southern Sierra Nevada batholith, California. *Geology*, 8(2), p. 314–341; doi:10.1130/GES00740.1, 2012.

Connolly, J.A.D., The geodynamic equation of state: what and how. *Geochemistry, Geophysics, Geosystems*, 10, Q10014l; doi:10.1029/2009GC002540, 2009.

Dimanov, A. & G. Dresen, Rheology of synthetic anorthite-diopside aggregates: Implications for ductile shear zones. *Journal of Geophysical Research: Solid Earth*, 110(B7), 2005.

Gerbi, C., et al., Effect of phase morphology on bulk strength for power-law materials, *Geophysical Journal International* 200.1, 374-389, 2015.

Handy, M.R., Flow laws for rocks containing two non-linear viscous phases: a phenomenological approach, *Journal of Structural Geology* 16.3, 287-301, 1994.

Hauksson, E., and M.-A. Meier, Applying depth distribution of seismicity to determine thermo-mechanical properties of the seismogenic crust in Southern California: Comparing lithotectonic blocks, *Pure Appl. Geophys.*, https://doi.org/10.1007/s00024-018-1981, 2018.

Hirth, G. & D. Kohlstedt (2003). Rheology of the upper mantle and the mantle wedge: A view from the experimentalists. *Inside the subduction Factory*, 83-10

Hirth, G., C. Teyssier, & J. W. Dunlap. An evaluation of quartzite flow laws based on comparisons between experimentally and naturally deformed rocks. *International Journal of Earth Sciences*, 90, 77-87, 2001.

Huet, B., P. Yamato, & B. Grasemann. The Minimized Power Geometric model: An analytical mixing model for calculating polyphase rock viscosities consistent with experimental data. *Journal of Geophysical Research: Solid Earth*, 119(4), 3897-3924, 2014.

Rybacki, E., M. Gottschalk, R. Wirth, & G. Dresen. Influence of water fugacity and activation volume on the flow properties of fine-grained anorthite aggregates. *Journal of Geophysical Research: Solid Earth*, 111, 2006.

Shinevar, W.J., M.D. Behn, & G. Hirth, Compositional dependence of lower crustal viscosity, *Geophys. Res. Lett.*, 42, 8333-8340, doi:10.1002/2015GL065459, 2015.

Shinevar, W.J., M.D. Behn, G. Hirth, and O. Jagoutz, Inferring Crustal Viscosity from Seismic Velocity: Application to the Lower Crust of Southern California, *Earth, Planet. Sci. Lett.*, https://doi.org/10.1016/j.epsl.2018.04.055, 494, 83-91, 2018.

Tullis, T.E., F.G. Horowitz, and J. Tullis, Flow laws of polyphase aggregates from end-member flow laws, *Journal of Geophysical Research,* 96, 8081-8096, 1991.

Zoback, M., Zoback, M. D., Townend, J., & Townend, J., Implications of hydrostatic pore pressures and high crustal strength for the deformation of intraplate lithosphere. *Tectonophysics*, 336(1-4), 19–30. doi:10.1016/S0040-1951(01)00091-9, 2001.